

SUPPLEMENTARY TABLE 1A
Oligonucleotides used for DNA binding substrates

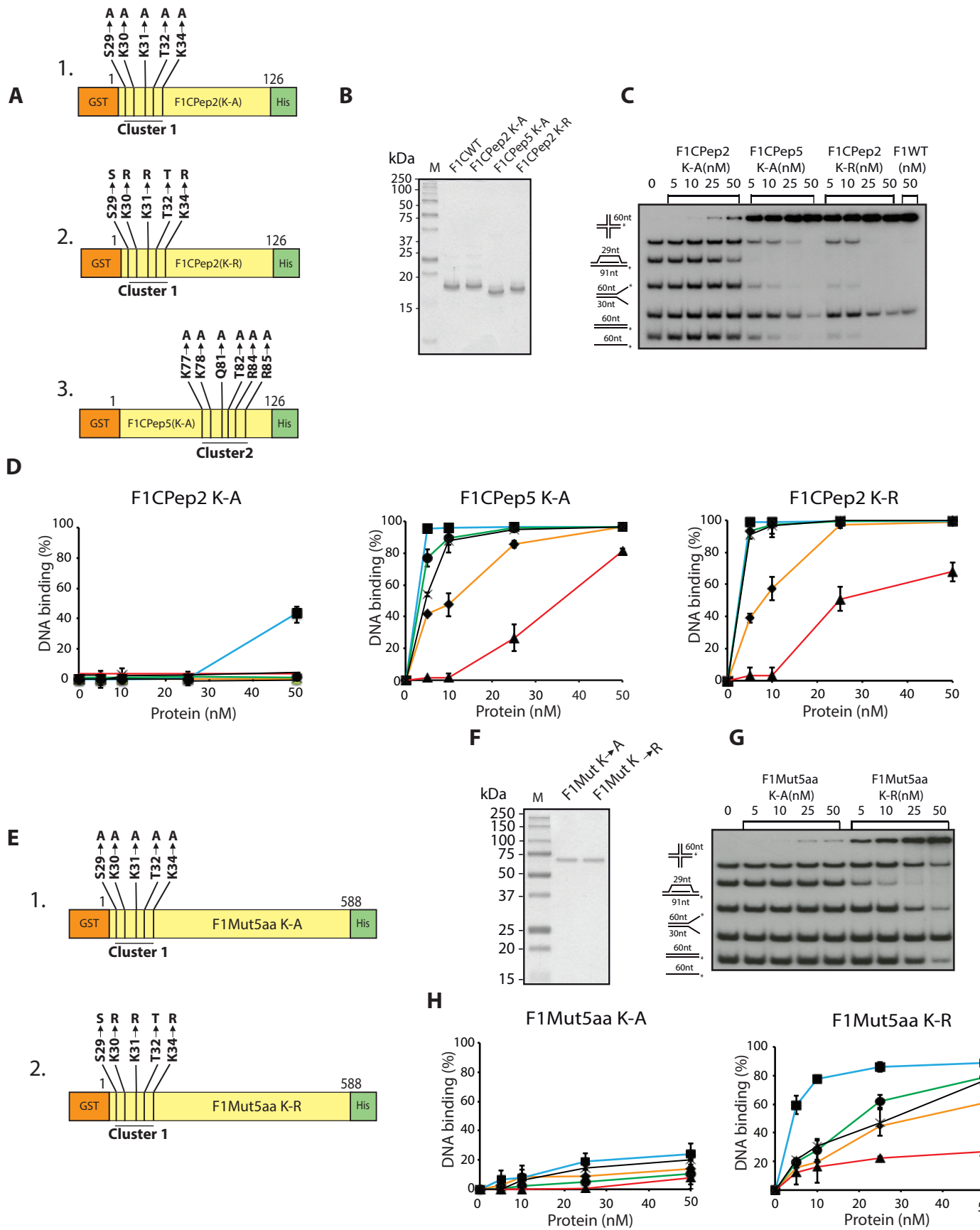
Oligonucleotide name	DNA sequences (5' to 3')
JYM925	GGGTGAAACCT GCAGGTGGGC AAAGATGTCC TAGCAATGTA ATCGTCAAGC TTTATGCCGT
JYM926	ACGCTGCCGA ATTCTACCAG TGCCAGCGAC GGACATCTT GCCCACCTGC AGGTTCACCC
JYM927	ACGGCATAAA GCTTGACGATT ACATTGCTAC ATGGAGCTGT CTAGAGGATC CGACTATCG
JYM928	CGATAGTCGG ATCCTCTAGA CAGCTCCATGG TCGCTGGCAC TGGTAGAATT CGGCAGCGT
JYM945	ACGGCATAAA GCTTGACGAT TACATTGCTA GGACATCTT GCCCACCTGC AGGTTCACCC
JYM1395	GCCAGGGACG GGGTGAAACCT GCAGGTGGGC GGCTGCTCAT CGTAGGTTAG TATCGACCT ATTGGTAGAAT TCGGCAGCGTC ATGCGACGGC
JYM1396	GCCGTCGCAT GACGCTGCCG AATTCTACCA CGCTACTAGG GTGCCTGCT AGGACATCTT TGCCCCACCTG CAGGTTCACCC CCGTCCCTGGC

SUPPLEMENTARY TABLE 1B
DNA binding substrates

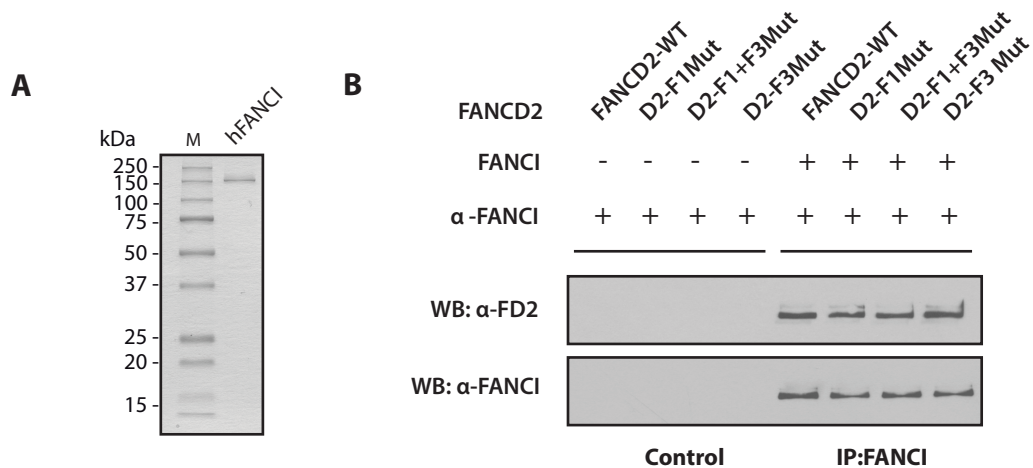
Structures	Oligonucleotide used
SS DNA	JYM 925
DS DNA	JYM 925, JYM 945
SA	JYM 925, JYM 926
D-loop	JYM 1745, JYM 1395 and JYM 1396
HJ	JYM 925, JYM 926, JYM 927 and JYM 928

SUPPLEMENTARY TABLE 2
Summary of DNA binding screen

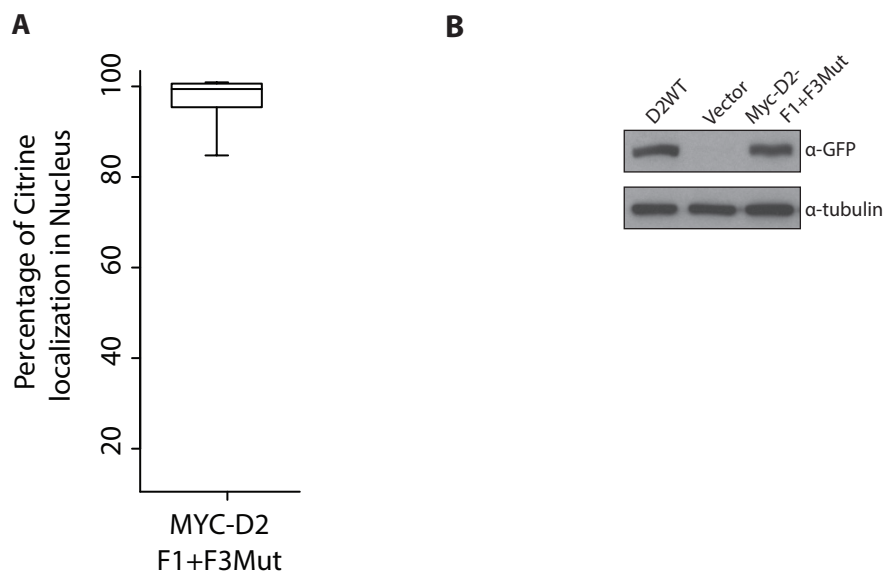
Peptide	Number of Substituent Mutations	Residues Substituted	Effect on DNA binding
F1-C (aa1 to 126)	-	-	++
F1-E (aa 1 to 49)	-	-	++
F1-F (aa 50 to 126)	-	-	+
F1-E peptide 2 mutated	8 aa	R24A ; K25A ; Q26A ; S29A ; K30A ; K31A ; T32A ; K34A	-
F1-C Mut Pep2 8aa	8 aa	R24A ; K25A ; Q26A ; S29A ; K30A ; K31A ; T32A ; K34A	-
F1-C : Peptide 5	6 aa	K77A; K78A ; Q81A ; T82A ; R84A ; R85A	+
F1-C Mut Pep2+Pep5	14 aa	R24A; K25A; Q26A; S29A; K30A; K31A; T32A; K34A K77A; K78A; Q81A; T82A; R84A ; R85A	-
F1 peptide 2 mutated	4 aa	S29A; K30A; K31A; T32A	+
F3-A (aa 841 to 1004)	-	-	++
F3-B (aa 1005 to 1178)	-	-	+
F3: Pep2+Pep10 mutated	11 aa	K861A; R863A; K864A; K865A; K867A, K992A; N993A; K994A; S996A; R997A; N998A	-
F3 : peptide 2	5 aa	K861A; R863A; K864A; K865A; K867A	-
F3 : peptide 2	3 aa	R863A; K864A; K865A	-
F3 : peptide 2	1 aa	K865A	-
F3 : peptide 10	6 aa	K992A; N993A; K994A; S996A; R997A; N998A	+



Supplementary Figure 1. Charge dependant DNA binding of residues in Cluster1. (A) Diagram representation indicating point mutations generated by site-specific mutagenesis. Cluster2 represents the mutations done in F1Cpep5 K-A. (B) Coomassie blue stained gel of purified F1CWT (18 kDa), F1Cpep2 K-A , F1Cpep5 K-A and F1Cpep2 K-R proteins. M, Molecular mass marker. (C) DNA binding activity of F1CWT, F1Cpep2 K-A , F1Cpep5 K-A and F1Cpep2 K-R to various recombinant DNA substrates. The percentage of DNA probes shifted were quantified by phosphorimaging and shown in (D). (E) Diagram representation of F1Mut5aa K-A (1) and F1Mut5aa K-R (2) mutants indicating point mutations generated by site-specific mutagenesis. Bold characters represent the substitutive mutations. (F) Purified F1Mut5aa K-A(66 kDa), F1Mut5aa K-R (66 kDa) proteins. M, Molecular mass marker. (G) DNA binding activity of F1Mut5aa K-A and F1Mut5aa K-R to various recombinant DNA substrates and DNA binding quantification (H) Error bars indicate S.E from three independently performed experiments.



Supplementary Figure 2: Interaction of FANCD2 WT and mutant proteins with FANCI. (A) The Coomassie blue stained gel of purified His10-tagged FANCI protein. M, Molecular mass marker. (B) Purified Human FANCI and equimolar concentrations of purified full-length FANCD2WT, D2-F1Mut, D2-F3Mut, or D2-F1+F3Mut were subjected to immunoprecipitation analysis. Immunoprecipitations with anti-FANCI antibody was performed and immune complexes were immunoblotted with anti-FANCD2 and anti-Histidine antibody, as indicated.

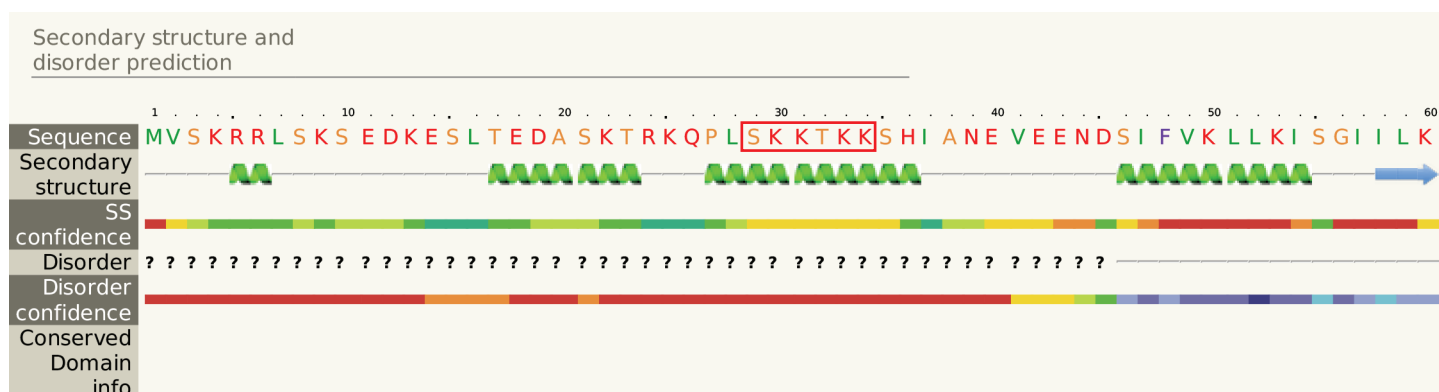


Supplementary Figure 3: (A) **Localisation of MYC-D2-F1+F3Mut.** A total of seventy-five FA-D2 cells expressing MYC-D2-F1+f3Mut were scored and box plotted for percentage of citrine expressed in the nucleus. (B) **Western blot showing comparable expression of D2WT and MYC-D2-F1+F3Mut in PD20 cells employed in Fig. 8E, F, and G.**

H. sapiens	1-MVSKRRLSKSEDK-ESLTEDASKTRKQPL--- SKKTKKSHIANEVEEND
B. taurus	1-MVSKRRLSKSEDK-ESLTEDASKTRKQPL--- SKKTKKSHIANEVEEND
P. troglodytes	1-MISKRKLSVSENK-ESLTEDASEARKQPL--- SKKTKKSHVHNEVEEND
M. musculus	1-MISKRRRLDSEDK-ENLTEDASK--TMPL--- SKLAKKSHNSHEVEENG
G. gallus	1-MVSKRKLSKIDAAEESSKTDLQS--RCPETKR SRISDKRAPSQGGLENE
X. laevis	1-MVAKRKLSRSDDREESFTADTSKNKKCRT--- SSKKSKALPQDGVVEND

H. sapiens	835-DYVPPLGNFDVETLDITPHTVTAISAK-IRK KGKIERKQKTDGSKTS
B. taurus	835-DYVPPLGNFDVETLDITPHTVTAISAK-IRK KGKIERKQKTDGSKTS
P. troglodytes	835-DYVPPLANFDLETLEETPHTSTAVAKI-RMKGKTGGKKRKADGGKTS
M. musculus	832-DYVPPFASVLDLTLDMMPRSSSAVAAKNRNKGKTGGKKQKADSNKAS
G. gallus	837-GYVPPPATFDSEAPEGVPSINAGG----PVR KK -NGKKRKSDSSKAC
X. laevis	834-GYIPSSAHFDSEPQEVLPSAIAPA---PAK AKKGKTPKSAGSKNA

Supplementary Figure 4: DNA binding residues are evolutionary conserved. A ClustalW multiple alignment of the DNA binding residues and the NLS of FANCD2 exhibits evolutionary semiconserved pattern, indicated by red and green colour bold letters.



Supplementary Figure 5: The N-terminal of FANCD2 has tendency to form helical structure. A Phyre2 protein secondary structure prediction algorithm of the N-terminal residues in FANCD2 indicates its propensity to form the α -helical secondary structure. DNA binding/NLS residues are depicted by the red box.

